Title
Effects of Composition and Structure of Mg/Al Oxides on Their Activity and Selectivity for the Condensation of Methyl Ketones

Journal
Industrial & Engineering Chemistry Research, 55(40)

ISSN
0888-5885

Authors
Shylesh, Sankaranarayanapillai
Kim, Daeyoup
Gokhale, Amit A
et al.

Publication Date
2016-10-12

DOI
10.1021/acs.iecr.6b03601

Peer reviewed

I&EC research
Industrial & Engineering Chemistry Research

Article

pubs.acs.org/IECR

Effects of Composition and Structure of Mg/Al Oxides on Their Activity and Selectivity for the Condensation of Methyl Ketones

Sankaranarayanapillai Shylesh,[†,‡] Daeyoup Kim,[‡] Amit A. Gokhale,[§] Christian G. Canlas,[∥] Jochem O. Struppe,[⊥] Christopher R. Ho,[‡] Deepak Jadhav,[†] Alice Yeh,[†] and Alexis T. Bell*[,†,‡]

[†]Energy Biosciences Institute and [‡]Department of Chemical and Biomolecular Engineering, University of California, Berkeley, California 94720, United States

[§]BASF Coorporation, 33 Wood Avenue South, Iselin, New Jersey 08830, United States

[∥]KAUST NMR Laboratory, King Abdullah University of Science and Technology, Thuwal 23955-6900, Saudi Arabia

[⊥]Bruker Biospin Coorporation, Billerica, Massachusetts 01821, United States

Supporting Information

ABSTRACT: The effects of chemical composition and pretreatment on Mg−Al hydrotalcites and alumina-supported MgO were evaluated for the gas-phase, self-condensation reaction of C_3−C_5 biomass-derived methyl ketones. We show that the selectivity toward the acyclic dimer enone and the cyclic enone trimer can be tuned by controlling the temperature of hydrotalcite calcination. Methyl ketone cyclization is promoted by Lewis acidic sites present on the hydrotalcite catalysts. XRD and thermal decomposition analysis reveal that the formation of periclase MgO starts above 623 K accompanied by complete disappearance of the hydrotalcite structure and is accompanied by an increase in hydroxyl condensation as the formation of well-crystallized periclase. ^{27}Al MQMAS and ^{25}Mg MAS NMR show that at progressively higher temperatures, Al^{3+} cations diffuses out of the octahedral brucite layers and incorporate into the tetrahedral and octahedral sites of the MgO matrix thereby creating defects to compensate the excess positive charge generated. The oxygen anions adjacent to the Mg^{2+}/Al^{3+} defects become coordinatively unsaturated, leading to the formation of new basic sites. A kinetic isotope effect, k_H/k_D = 0.96, is observed at 473 K for the reaction of $(CH_3)_2CO$ versus $(CD_3)_2CO$, which suggests that carbon−carbon bond formation leading to the dimer aldol product is the rate-determining step in the condensation reaction of methyl ketones. We also show that acid−base catalysts having similar reactivity and higher hydrothermal stability to that of calcined hydrotalcites can be achieved by creating defects in MgO crystallites supported alumina as a consequence of the diffusion of Al^{3+} cations into MgO. The physical properties of these materials are shown to be very similar to those of hydrotalcite calcined at 823 K.

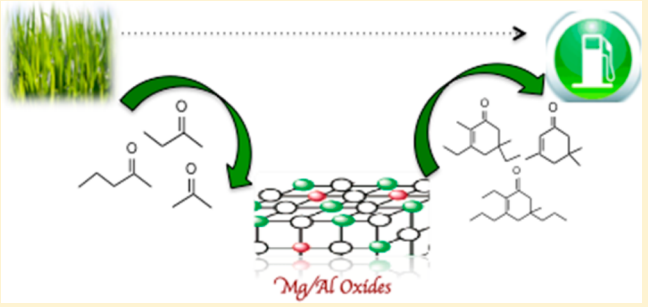

INTRODUCTION

Biomass-derived ketones and aldehydes can be used as synthons to form carbon−carbon bonds in compounds needed for chemical intermediates and transportation fuels.[1,2] Although cross-condensation of aldehydes, such as hydroxymethyl furfural (HMF) or furfural (FUR), with acetone has been discussed extensively,[2] the self-condensation of alkyl methyl ketones to produce fuel precursors is a fairly recent innovation.[3−5] We have recently discussed various strategies for sourcing alkyl methyl ketones (MKs) from renewable sources using different chemical pathways as well as hybrid biological-chemical pathways, as illustrated in Scheme 1.[6,7] For example, propan-2-one (acetone) can be produced from an acetone-butanol-ethanol (ABE) mixture produced by the Clostridial fermentation of sugars or from the bio-oil obtained by fast pyrolysis of biomass feed stocks.[2,7] Butan-2-one can be obtained in more than 90% selectivity by aqueous-phase, acid-catalyzed dehydration of 2,3-butane diol (2,3-BDO) or by the decarboxylation of levulinic acid.[8−10] Finally, pentan-2-one can be produced by the ring opening hydrogenolysis of 2-methylfuran or by the monoalkylation of acetone with ethanol derived from an ABE mixture (Scheme 1).[4,7]

Condensation reactions of short chain aldehydes and ketones are required to increase the carbon chain length and to decrease the O:C ratio and energy density of the final product.[11−13] These reactions have conventionally been promoted by homogeneous base catalysts such as NaOH or KOH; however, these catalysts cannot be readily separated from the reaction mixture and are difficult to dispose of.[14,15] We have recently shown that calcined hydrotalcite, HT, is an active and highly selective heterogeneous catalyst for the self- and cross-condensation of biomass-derived C_4−C_{11} methyl ketones to

Received: September 17, 2016
Accepted: September 22, 2016
Published: September 22, 2016

DOI: 10.1021/acs.iecr.6b03601
Ind. Eng. Chem. Res. 2016, 55, 10635−10644

Scheme 1. Synthesis of Various Methyl Ketones by Hybrid Chemical-Biological Pathways

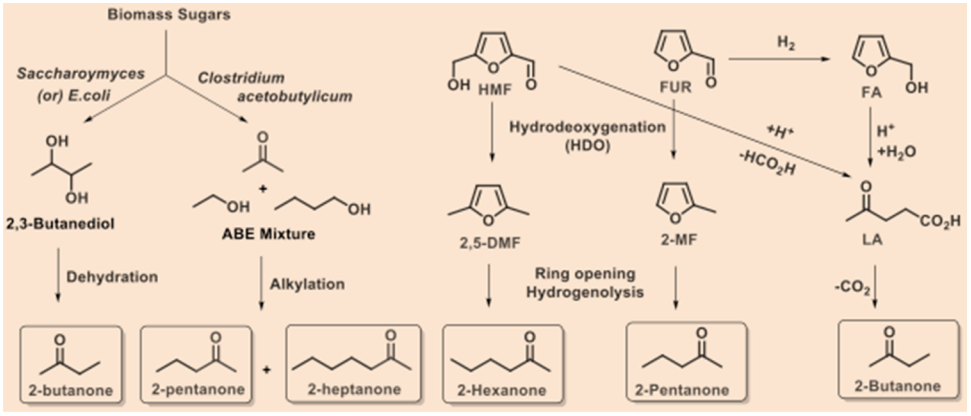

produce cyclic enones, which upon subsequent hydrodeoxygenation produce cyclic alkanes that have properties making them suitable for aviation fuel and lubricants.[6,13,16,17]

Hydrotalcite-type layered double hydroxides (LDHs) are inorganic compounds with the chemical composition $M^{2+}_{1-x}M^{3+}_{x}(OH)_2(A_{x/n})^{n-}\cdot yH_2O$, where M^{2+} and M^{3+} are divalent and trivalent metal cations, x is the molar ratio of the trivalent cation $[M^{3+}/(M^{2+} + M^{3+})]$ which can be varied between 17 and 33%, and A^{n-} is an anion with charge n, most often a carbonate ion.[16] The structure of these materials is similar to that of brucite, $Mg(OH)_2$, where magnesium is octahedrally surrounded by six oxygens in the form of hydroxides with the octahedral units forming infinite sheets through an edge sharing. The presence of trivalent cations like Al^{3+} in the lamellar sheet induces an overall positive charge, which is compensated by the presence of intercalated anions together with water.[17] In as-synthesized hydrotalcite, Al has six Mg atoms at nearest neighboring positions, connected through OH groups, whereas Mg has both Al and Mg at these positions.[18,19]

Once calcined at elevated temperatures, hydrotalcites become effective catalysts for various carbon−carbon bond forming reactions, such as aldol, Knoevenagel, Michael, and Claisen-Schmidt condensation.[16,17,20−24] The catalytic competence of hydrotalcites after calcination is a result of the high surface area and moderate acidity/basicity of the resultant Mg−Al mixed oxides.[27] However, calcined hydrotalcites are known to be quite susceptible to deactivation by water.[17] Although acid−base character is essential for the catalytic activity of hydrotalcite-type catalysts, the relationship between catalytic activity, chemical composition, and the structural stability issues of calcined hydrotalcites in the presence of water remain elusive in the catalytic upgrading reaction of bioderived methyl ketones.

The aim of the present study was to establish the changes occurring during the calcination of HT and, in particular, how the calcination temperature affects the distribution of acid and basic sites and the performance of calcined HT for promoting the self-condensation of C_3−C_5 methyl ketones.[16,17] We found that hydrotalcites calcined at 623 and 1273 K are selective for ketone dimerization, whereas hydrotalcites pretreated at 823 K and an MgO supported alumina are selective for the trimerization of methyl ketones to cyclic enones. A further goal of our work was to identify means for achieving the desired properties of calcined HT while reducing the susceptibility of this material to deactivate upon exposure to water, a product of methyl ketone condensation. This goal was further pursued by examining the properties of a MgO-supported Al_2O_3. The structure of this material following calcination is very similar to that to calcined HT, as is its catalytic activity for methyl ketone condensation. A notable finding is that MgO-supported Al_2O_3 is structurally more stable and robust than calcined hydrotalcite in the presence of water.

EXPERIMENTAL SECTION

Synthesis of Hydrotalcite (HT). Mg−Al HT (Mg/Al = 3) was prepared by coprecipitation from a solution of Mg and Al nitrates.[16,17] In a typical synthesis procedure, $Al(NO_3)_3\cdot 9H_2O$ (50 mmol) and $Mg(NO_3)_2\cdot 6H_2O$ (150 mmol) were dissolved in deionized water (100 mL). This solution was slowly added to an aqueous solution containing Na_2CO_3 (60 mmol) and NaOH (210 mmol). The resulting mixture was heated at 353 K for 24 h with vigorous stirring. The white slurry obtained was then cooled to room temperature, filtered, washed with large amount of deionized water, and dried overnight at 383 K. The dried material was then calcined at various temperatures to produce the final crystalline hydrotalcite catalysts. For instance, hydrotalcite calcined at 823 K is designated as HT@823 K. ICP elemental analysis showed that at an Mg/Al molar ratio of 3 the hydrotalcite sample contained 42.2 wt % Mg and 14.2 wt % Al. MgO supported Al_2O_3 was prepared by incipient wetness impregnation using magnesium nitrate as the precursor at an Mg/Al ratio of approximately 3. The supported catalyst was then dried in a vacuum oven at 383 K and then calcined in air at 823 K for 5 h. The calcined sample is denoted as (Mg/Al)O in the manuscript.

Characterization. Powder X-ray diffraction (PXRD) patterns were acquired using a Bruker D8 GADDS diffractometer equipped with a Cu−Kα source (40 kV, 40 mA). Brunauer−Emmet−Teller (BET) surface areas were determined from nitrogen adsorption isotherms obtained using a Micromeritics Gemini VII 2390 surface area analyzer. The Mg/Al ratio of hydrotalcites was determined by ICP-OES using an Optima 7000 DV instrument. Infrared spectra were acquired using a Thermo Scientific Nicolet 6700 FTIR spectrometer equipped with a liquid-nitrogen-cooled MCT detector. Each spectrum was obtained by averaging 32 scans taken with 1 cm^{-1} resolution. 0.05 g of catalyst was pressed into a 20 mm-diameter pellet (<1 mm thick) and placed into a custom-built transmission cell equipped with CaF_2 windows, a K-type thermocouple for temperature control, and resistive cartridge heaters.

DOI: 10.1021/acs.iecr.6b03601
Ind. Eng. Chem. Res. 2016, 55, 10635−10644

^{27}Al 1-D magic angle spinning (MAS) and ^{27}Al 2-D multiple quantum MAS (MQMAS) NMR spectra were acquired out using a 500 MHz (11.7 T) Bruker Avance I NMR spectrometer. This instrument is equipped with a standard bore H/X magic angle spinning probe, which uses 4 mm o.d. zirconia rotors that rotate at speeds between 11 and 13.5 kHz. All ^{27}Al spectra were referenced to $Al(NO_3)_3$ in D_2O at 0 ppm. To resolve the 1-D ^{27}Al signals further, two-dimensional multiple quantum MAS (MQMAS) experiments were performed using the soft pulse added mixing (SPAM) technique for sensitivity enhancement and with rotor synchronization or with half-rotor synchronization depending on the required spectral window in the F1 dimension. The pulses used for excitation and conversion were optimized individually for each sample. The 2-D spectra were processed by doing a 2-D Fourier transformation with a shearing transformation. 1-D ^{25}Mg MAS NMR at 30.61 MHz was obtained on a 500 MHz Bruker Avance NMR spectrometer equipped using a Hahn echo sequence with a low gamma probe.

The elemental composition of the support material was determined by scanning transmission electron microscopy with energy dispersive spectroscopy (STEM-EDS). Elemental mapping by STEM-EDS was done using an FEI Titan electron microscope located in the Molecular Foundry at the Lawrence Berkeley National Laboratory. The microscope was operated at an accelerating voltage of 200 kV, and fluorescent X-rays with energies between 0 and 40 kV were collected using a 4-segment silicon drift detector. The catalyst composition was quantified using the Bruker Esprit software program with the Cliff-Lorimer method using the O Kα (0.525 keV), Mg Kα (1.254 keV), and Al Kα (1.739 keV) peaks.

Reaction Studies. The gas-phase reaction of C_3-C_5 methyl ketones (MKs) carried out in a 6.35 mm OD (~4 mm ID) quartz tube containing an expanded section (~12.7 mm OD, ~ 20 mm length). The reactor was packed with quartz wool above and below the catalyst bed to hold the catalyst in place. MK was injected into a He flow using a syringe pump. Catalysts were pretreated in He at 473 K for 2 h before being contacted with the feed. Experiments were carried out at 473−573 K, total gas pressures of 1 atm, and a total gas flow rate of 150 cm^3 min^{-1}. All the results reported were obtained after 120 min time on stream. Reaction products were analyzed using an Agilent 6890N gas chromatograph containing a bonded and cross-linked (5%-phenyl)-methyl polysiloxane capillary column (Agilent, HP-1) connected to a flame ionization detector.

RESULTS AND DISCUSSION

Characterization. XRD patterns of the hydrotalcite sample (HT, Mg/Al = 3) acquired after different pretreatment procedures are shown in Figure 1 together with those for the reference compounds MgO, Al_2O_3, and (Mg/Al)O. The XRD pattern of as-synthesized hydrotalcite shows sharp diffraction peaks at 2θ = 11.0, 22.2, 34.2, 38.2, 45.1, 59.9, and 61.3 corresponding to the well-crystallized, layered structure of hydrotalcites.[16] Calcination at 623−823 K leads to collapse of the layered structure and the appearance of three broad ill-defined peaks at 2θ = 36.9, 42.7, and 62.3 corresponding to the fcc form of MgO (periclase).[17] No traces of hydrotalcite peaks were detected after the calcination at 623 K. It is also noted that the XRD patterns give no indication for the presence of additional Al_2O_3, which suggests that the alumina present may be too amorphous to be detected by XRD. However, the

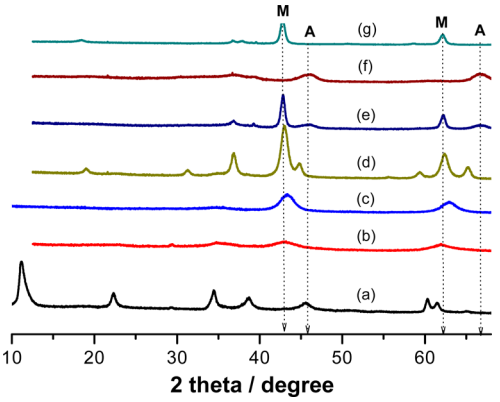

Figure 1. XRD patterns of hydrotalcite pretreated at different temperatures and various reference samples: (a) HT@373 K, (b) HT@623 K, (c) HT@823 K, (d) HT@1273 K, (e) (Mg/Al)O, (f) γ-Al_2O_3, and (g) MgO. M = MgO and A = γ-Al_2O_3.

diffraction peaks for MgO observed after calcining HT have higher 2θ values than those of pure MgO, suggesting that Al^{3+} cations have incorporated into the MgO lattice.[25] Upon calcining the sample to 1273 K, well-defined XRD peaks appear at 2θ = 19.0, 31.0, 36.9, 59.4, and 65.2 characteristic of $MgAl_2O_4$ spinel and periclase MgO. These results are consistent with previous reports that MgO and Al_2O_3 can react to form spinels when heated above 873 K.[26] The XRD pattern of (Mg/Al)O is presented in Figure 1e. Peaks characteristic of γ- Al_2O_3 and the periclase form of MgO are clearly evident which is different from the periclase structure obtained with hydrotalcite pretreated at 823 K (Figure 1c).

The thermal decomposition of layered hydrotalcite (Mg/Al = 3) to the MgO periclase structure was characterized by thermal (TG-DTG) analysis. Figure S1 shows that decomposition occurs in a stepwise process. The first weight loss, ~14%, occurs around 473 K, and a further weight loss, ~45%, occurs above 823 K. XRD patterns of hydrotalcite pretreated at 473 K retain the layered hydrotalcite structure, suggesting that the weight loss below 473 K is entirely due to removal of loosely bound water. Similarly, the total weight loss observed after calcining 823 K is similar to that calculated from the weight taken before and after calcination. These results suggest that approximately 30% of the total weight loss is accounted for by the loss of carbonate anions and hydroxyl groups. Consistent with the TGA pattern, DTG data shows a large endothermic peak at 473 K corresponding to the loss of interlayer water, a second endothermic peak at 563−623 K corresponding to the combined loss of structural hydroxyl groups and carbonate species, and the final loss around 683 K arises due to further condensation of hydroxyl groups (Figure 2).[28] Dehydroxylation collapses the layered structure of hydrotalcite leading to the formation of the MgO above 613 K. Previous studies suggest that the dehydroxylation begins within brucite layers and then occurs in a second stage between adjacent layers causing collapse of the structure.[29] Thus, the transformation of hydrotalcites to Mg−Al mixed oxides occurs through the controlled thermal decomposition involving a series of reactions, involving dehydration, decarboxylation of the interlayer carbonates, and dehydroxylation of the hydroxyl groups present in the brucite layers. It is also notable that the removal of water and gaseous products from the hydrotalcite sample during calcination creates porosity in the MgO crystals and thereby leads to an increase in surface area (Figure S2).

DOI: 10.1021/acs.iecr.6b03601
Ind. Eng. Chem. Res. 2016, 55, 10635−10644

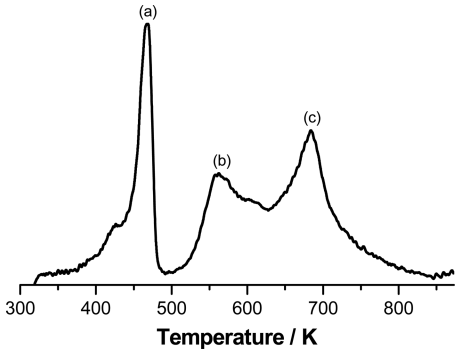

Figure 2. Thermal decomposition patterns of an as-synthesized hydrotalcite (HT, Mg/Al = 3) catalyst: Peaks for (a) dehydration, (b) decarboxylation, and (c) dehydroxylation.

Further spectroscopic characterization was carried out in order to understand the local structure of aluminum and magnesium present on the hydrotalcite samples pretreated at various temperatures. As seen in Figure 3a, one-dimensional

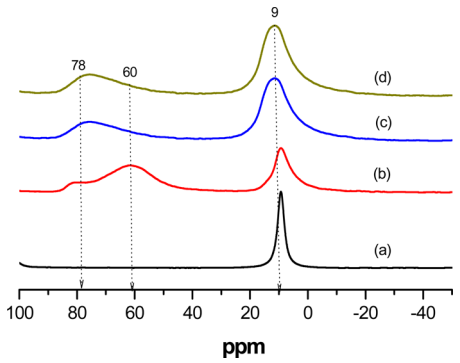

Figure 3. One-dimensional ^{27}Al MAS NMR of hydrotalcite (HT, Mg/Al = 3) pretreated at different temperatures: (a) 373 K, (b) 623 K, (c) 823 K, and (d) (Mg/Al)O pretreated at 823 K.

(1D) ^{27}Al MAS NMR of as-synthesized hydrotalcite (Mg/Al = 3) shows the presence of a single, sharp ^{27}Al signal at 9 ppm characteristic of octahedral (O_h) AlO_6 coordination.[30] This result is consistent with previous reports that as-synthesized hydrotalcite consists of positively charged brucite-like layers due to the presence of trivalent cation such as Al^{3+} in octahedral units between the lamellae.[17] With an increase in the calcination temperature, a progressive decrease in the intensity of the octahedral peak is noted. The sample pretreated at 623 K (Figure 3b) shows relatively broad signals at 10 ppm and the appearance of Al in two different tetrahedral (T_d) coordination sites as revealed by the peaks at 60 and 78 ppm.[22] Treating the sample at 823 K (Figure 3c) produces a very broad peak at 10 ppm, suggesting distorted octahedral aluminum, and another broad peak at 78 ppm, suggesting the presence of tetrahedral aluminum. The absence of peaks near 30 ppm suggests the absence of five-coordinated aluminum during the transition of aluminum from O_h to T_d coordination. The distribution of O_h and T_d Al^{3+} can be estimated by integrating the areas under the corresponding peaks. The ratio of Al_O/Al_T in the hydrotalcite samples decreases in the following order with increasing calcination temperature: 100/0 (373 K) > 65/35 (623 K) > 55/45 (823 K) consistent with the transition of Al^{3+} from the O_h to the T_d sites.[28] Thus, Al^{3+} cations occupy the octahedral positions in HT before calcination, and upon calcination the Al cations move from octahedral to tetrahedral positions. The ^{27}Al NMR spectrum of (Mg/Al)O calcined at 823 K (Figure 3d) exhibits the presence of a peak at 9 ppm for Al^{3+} in octahedral sites and another peak at 75 ppm for Al^{3+} in tetrahedral sites with an Al_O/Al_T ratio of 1.3. It is notable that this spectrum is very similar to that obtained for HT calcined at 823 K.

The peak broadening seen in the ^{27}Al NMR spectra of hydrotalcite pretreated at high temperatures can be due to the overlapping signals, increased nonsymmetry, or increased second-order quadrupolar couplings.[31] To resolve the Al signal further and to clearly understand the local structure of the Al^{3+} cations, the samples were analyzed by two-dimensional ^{27}Al multiple quantum-magic angle spinning (MQ-MAS) NMR spectroscopy (Figure 4). The MQMAS experiment for half

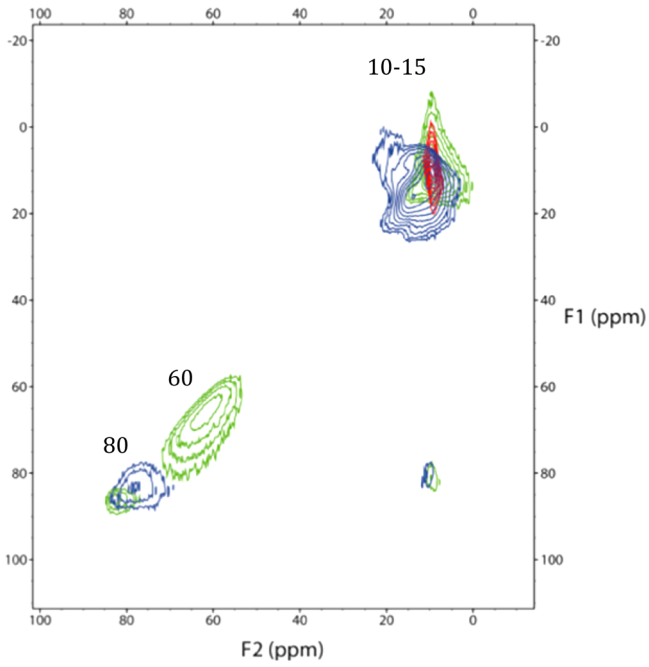

Figure 4. ^{27}Al multiple quantum-magic angle spinning (MQ-MAS) NMR spectroscopy of hydrotalcites pretreated at different temperatures: HT@373 K (red), HT@623 K (green), and HT@823 K (blue).

integer quadrupolar nuclei is a powerful technique to separate anisotropic interactions from isotropic interactions.[31,32] The MQMAS sheared spectrum of as-synthesized hydrotalcite (Mg/Al = 3) exhibits a single peak at 10 ppm for an Al^{3+} in an octahedral site ($Al(OH)_6$). The sharpness of the peak is reflective of the high symmetry of this site and suggests that Al cations in hydrotalcite are not randomly distributed in the layered structure but are arranged in a ordered fashion. The presence of a single aluminum site suggests the chemical similarity of the Al species present on the as-synthesized hydrotalcite sample.[33] After calcination at 623 K, the MQMAS-sheared spectrum shows distinct spectral differences. A major broad feature around 10 ppm due to aluminum in an octahedral site is present together with a minor peak at 15 ppm also due to Al^{3+} in an octahedral site, in addition to the presence of distinct peaks at 60 and 80 ppm for Al^{3+}in T_d sites. The cross peak is dispersed parallel to the F2 axis suggesting that the line width is mainly due to the second-order quadrupolar broadening. After calcination at 823 K, MQMAS-sheared spectra shows two well-resolved octahedral aluminum sites centered at 10 and 15 ppm.

DOI: 10.1021/acs.iecr.6b03601
Ind. Eng. Chem. Res. 2016, 55, 10635−10644

This sample also shows one well-resolved peak at 80 ppm for the tetrahedral aluminum site.[18]

The presence of another octahedral site at 15 ppm during pretreatments suggests the random insertion of Al^{3+} cations into octahedral sites of the periclase structure of MgO. The tetrahedral aluminum peak at 80 ppm evidently has a higher electron density and thereby can be assigned to Al_T−O bonded to Mg^{2+} (Al_T−O−Mg), while the 60 ppm peak can be assigned to Al_T−O bonded to Al (Al_T−O−Al).[34] Consistent with this finding, elemental mapping by STEM-EDS shows evidence for segregation of Al and Mg to the edges of the hydrotalcite crystals upon pretreatment at 623 K (Figure S3). Thus, upon calcination to 823 K, transitions from Al_O−O−Mg (10 ppm) to Al_T−O−Mg (80 ppm) occur, possibly through an intermediate aluminum state (Al_T−O−Al). The Al^{3+} insertion into the T_d and O_h sites produces the defect sites as cationic vacancies in the MgO framework are needed to compensate the positive change generated. As a consequence, the O^{2-} ions adjacent to the Mg^{2+} or Al^{3+} become coordinatively unsaturated, leading to the formation of new basic sites. Quantum calculations also suggest that the main factor influencing the generation of basicity in hydrotalcites is an increase in O^{2-} anions coordinated to the Mg^{2+}.[37] Thus, the number of defects and thereby the number of strong basic sites in the lattice of MgO should be expected to increase with an increase in hydrotalcite pretreatments.

The recording of ^{25}Mg MAS NMR spectra is particularly challenging because this isotope has a low gyromagnetic ratio, low natural abundance (~10%), and relatively large quadrupole moment. Previous studies suggest that as-synthesized hydrotalcite possesses a single axially symmetric $Mg(OMg)_6$ environment similar to that observed for pure brucite, $Mg(OH)_2$.[19] The one-dimensional ^{25}Mg MAS NMR spectrum of hydrotalcite pretreated at 623 and 823 K shows the presence of a single, relatively broad peak at 23 ppm, suggesting the formation of a poorly crystalline MgO phase (Figure S4).[28,35,36] However, due to the broadness of the spectrum it is difficult to conclude whether there is only one Mg environment or whether other resonances are hidden under the broad one pulse spectrum. The broadness of the ^{25}Mg peak compared to the ^{27}Al NMR suggests that Mg^{2+} has a much more distorted environment than Al^{3+}. Thus, the ^{25}Mg MAS NMR spectrum of calcined hydrotalcite strongly resembles MgO, suggesting that a MgO-like phase is formed after calcination, consistent with the deductions drawn from XRD data.

In situ IR studies were carried out using CO_2 as a probe molecule to probe the properties of the basic sites present on the catalyst surface. Figure 5 shows the infrared spectra of calcined hydrotalcite (HT@823 K), after CO_2 adsorption at room temperature and subsequent evacuation at various temperatures. The bands appearing at 1590−1540 cm^{-1} and 1400−1360 cm^{-1} are attributable to asymmetric and symmetric O−C−O stretching vibrations, respectively, of unidentate carbonate species formed on high-strength basic sites (O^{2-}).[31] CO_2 adsorption on Mg−O pairs having medium basicity produce bidentate carbonate species that have characteristic asymmetric and symmetric O−C−O vibrations near 1630−1610 cm^{-1} and 1350−1320 cm^{-1}; and finally, bicarbonate species formed by the reaction of CO_2 with weakly basic surface hydroxyl groups exhibit asymmetric and symmetric O−C−O stretching vibrations at 1670−1650 cm^{-1} and 1480−1420 cm^{-1}, respectively and C−OH bending mode vibrations at 1220 cm^{-1}.[38] All three forms of adsorbed CO_2

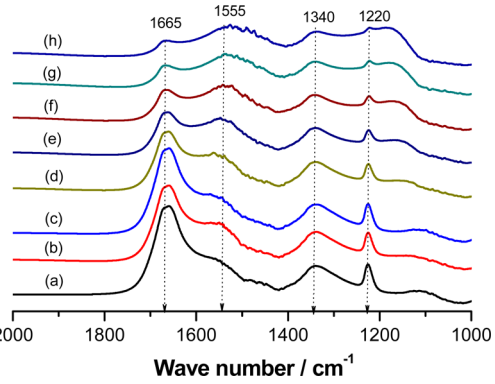

Figure 5. In situ FT-IR of calcined hydrotalcite (HT@823 K, Mg/Al = 3) after CO_2 adsorption at room temperature and desorption at various temperatures. (a) 298 K, (b) 323 K, (c) 373 K, (d) 423 K, (e) 473 K, (f) 523 K, (g) 573 K, and (h) 623 K.

were observed, reflecting the presence of strong (O^{2-}), medium (M−O), and weakly basic sites (−OH) on the surface of calcined hydrotalcite. Desorption of CO_2, by increasing the temperature from 573 K, resulted in complete disappearance of the weakly basic bicarbonate species; however, unidentate and bidentate carbonates remained up to 623 K, indicating the presence of moderately strong basic sites.

Figure S5 shows infrared spectra of calcined HT, (Mg/Al)O, γ-Al_2O_3, and MgO acquired after CO_2 adsorption at room temperature and evacuation at 473 K. All catalysts were pretreated at 823 K before the adsorption of CO_2. Similar to the calcined hydrotalcite, the spectrum of CO_2 adsorbed on (Mg/Al)O, and γ-Al_2O_3 exhibit bands at 1650, 1440, and 1340 cm^{-1}, characteristic of weak bicarbonate species and medium strength carbonate species, respectively. By contrast, MgO exhibits the presence of high strength unidentate carbonate species, as evidenced by the bands at 1570 and 1390 cm^{-1}. These result suggests that while calcined hydrotalcites and (Mg/Al)O possess predominantly medium to weakly basic sites, MgO possesses strongly basic sites. The strength of basic sites is known to follow the order isolated low coordinated O^{2-} ions > O^{2-} in metal−oxygen pairs > −OH groups.[38] Accordingly, the basicity determined from CO_2 IR follows the order MgO > HT ≈ (Mg/Al)O > γ-Al_2O_3.

The acidic properties of the calcined hydrotalcites were characterized by IR spectroscopy using adsorbed pyridine as a probe to distinguish between Lewis acid (L) and Brønsted acid (B) sites. In general, IR peaks at 1445, 1575, and 1600 cm^{-1} are attributed to strong Lewis acid sites; a peak at 1490 cm^{-1}, to a combination of Lewis and Brønsted acid sites; and peaks at 1540 and 1640 cm^{-1}, to Brønsted acid sites.[23,39] A peak at 1590 cm^{-1} is assigned to hydrogen-bonded pyridine molecules (H).[39] Figure S6 shows infrared spectra for calcined hydrotalcite, (Mg/Al)O, and the reference materials MgO and γ-Al_2O_3 acquired following pyridine adsorption at room temperature and evacuation at 473 K. IR spectra suggest that HT calcined at 823 K contains hydrogen-bonded pyridine and pyridine bonded to strong Lewis acid sites and no evidence for pyridine interacting with Brønsted acid sites. The absence of Brønsted acidic sites on hydrotalcites suggest that the residual hydroxyl groups are weakly acidic. The spectra for (Mg/Al)O and γ-Al_2O_3 show the presence of strong Lewis acid sites and the absence of Brønsted acid sites. By contrast, all of the IR bands for pyridine adsorbed on MgO occur at higher wave

DOI: 10.1021/acs.iecr.6b03601
Ind. Eng. Chem. Res. 2016, 55, 10635−10644

Scheme 2. Reaction Pathway for Propan-2-one Condensation over Acid−Base Catalysts

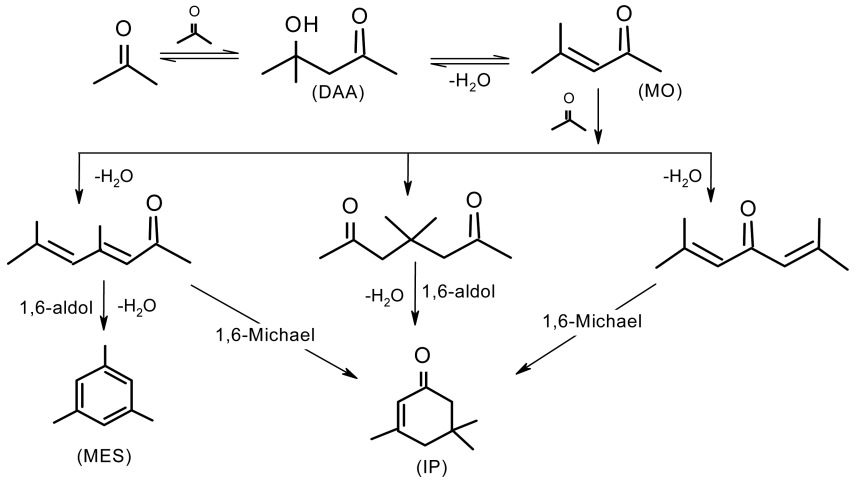

numbers, suggesting that the acidity of MgO is much weaker than that of γ-Al_2O_3, calcined hydrotalcite, or (Mg/Al)O.

The results presented above demonstrate that with pretreatment, the layered structure of as-synthesized hydrotalcites collapses to Mg−Al mixed oxides by decarboxylation and dehydroxylation reactions. During this transformation, Al^{3+} cations diffuse out of the octahedral brucite layers and incorporate into the tetrahedral and octahedral sites of the MgO matrix through an intermediate Al_T−O−Al aluminum state. The Al^{3+} insertion in MgO latice induces defects in the crystal to compensate the excess positive charge generated, leading to the formation of new basic sites. The number of defect sites and thus the number of basic sites increase with an increase in hydrotalcite pretreatment from 623 to 823 K. By contrast, XRD peaks characteristic of γ-Al_2O_3 and MgO are observed for (Mg/Al)O calcined at 823 K. The results of (Mg/Al)O characterization by ^{27}Al NMR and CO_2 IR show, however, similar Al_O/Al_T sites and basic sites, respectively, to those observed in HT@823 K. These results suggest that active sites similar to hydrotalcite pretreated at 823 K can be designed by introducing defect sites into MgO crystallites.

Catalysis. As noted in the Introduction, propan-2-one, butan-2-one, and pentan-2-one can be sourced from biomass by various chemical and/or biological routes (Scheme 1). Condensation of these compounds produces molecules that serve as precursors to transportation fuels.[6,7,12,13] A classic example of this type of carbon−carbon bond formation is the base-catalyzed dimerization of propan-2-one (acetone) to produce mesityl oxide (MO) or its trimerization to produce cyclic trimers isophorone (IP) and mesitylene (MES) as shown in Scheme 2.[40]

A comparison of activity of HT, (Mg/Al)O, MgO, and γ-Al_2O_3, calcined at 823 K, for the gas phase self-condensation of propan-2-one is shown in Figure 6. The product distributions vary considerably depending on the catalyst composition. Condensation over HT@823 K produces significant yields of IP but no aromatic compounds. Similarly, (Mg/Al)O produces IP with greater than 80% selectivity, the remainder of the product being MO and MES. By contrast, >90% of the product formed over MgO is mesityl oxide; however, this catalyst deactivates with time on stream, most likely due to the formation of higher condensation products that blocked the high strength basic sites.[41] We propose that further condensation of propan-2-one over MgO, but not over calcined

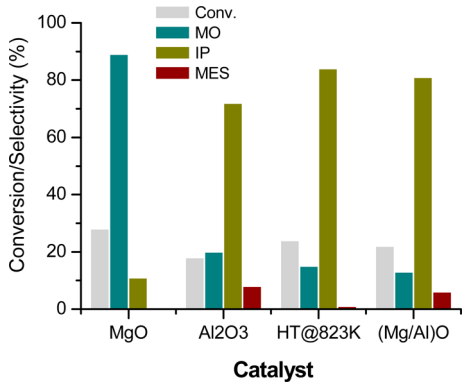

Figure 6. Comparison of different catalysts in the gas-phase condensation reaction of propan-2-one. Reaction conditions: T = 473 K, WHSV = 0.4 h^{-1}, M_{Cat} = 0.1 g, Q_{tot} = 150 cm^3 min^{-1}.

HT or (Mg/Al)O, is due to the absence of Lewis acid sites (LAS) on MgO, which are required to promote the reaction of phorones to IP via 1,6-Michael addition.[21] The conversion of propan-2-one over various catalysts correlates to the basicity determined from CO_2 IR measurements and follows the order MgO > HT ≈ (Mg/Al)O > γ-Al_2O_3 (Figure 6). Interestingly, γ-Al_2O_3 shows a high selectivity toward IP, comparable to that observed for hydrotalcites and (Mg/Al)O.[38,42] However, this catalyst showed the significant formation of an aromatic compound, mesitylene. The presence of mesitylene (MES) in the products formed over (Mg/Al)O and γ-Al_2O_3 indicates that strong LAS on γ-Al_2O_3 promote internal 1,6-aldol condensation as shown in Scheme 2.[40,41] A similar result is also noted by changing propan-2-one to butan-2-one (Figures S7 and S8). The results presented above thus suggest that basic catalysts such as MgO possessing strongly basic sites are less selective toward the formation of cyclic trimers, while Lewis acid−base catalysts such as calcined hydrotalcite and (Mg/Al)O exhibit a high selectivity to the cyclic enone trimer, IP.

The temperature at which hydrotalcite is calcined has a significant influence on its activity and selectivity to form cyclic trimers. As-synthesized hydrotalcites and hydrotalcites calcined up to 473 K are inactive for the condensation of propan-2-one. As shown in Figure 7, the catalytic activity of hydrotalcite increases by a factor of 2 as the calcination temperature is increased from 623 to 823 K but then drops when the

DOI: 10.1021/acs.iecr.6b03601
Ind. Eng. Chem. Res. 2016, 55, 10635−10644

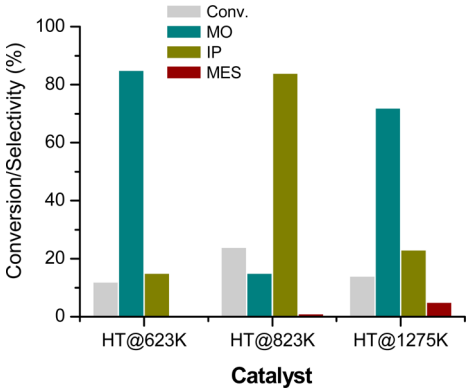

Figure 7. Catalytic activity of hydrotalcite pretreated at different temperatures in the self-condensation reaction of propan-2-one. Reaction conditions: T = 473 K, WHSV = 0.4 h^{-1}, M_{Cat} = 0.1 g, Q_{tot} = 150 cm^3 min^{-1}.

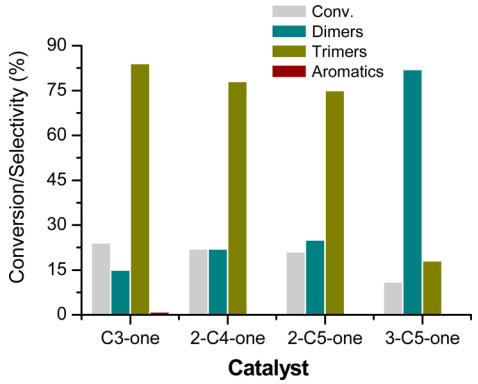

Figure 8. Self-condensation of various C_3−C_5 ketones in the presence of hydrotalcites calcined at 823 K. Reaction conditions: T = 473 K, WHSV = 0.4 h^{-1}, M_{Cat} = 0.1 g, Q_{tot} = 150 cm^3 min^{-1}.

temperature is raised to 1273 K. Hydrotalcite calcined at 623 K exhibits a selectivity of >80% mesityl oxide, MO, but raising the calcination temperature to 823 K changes the selectivity of IP to >80%.

The observed changes in activity and selectivity with calcination temperature are closely related to the changes in the catalyst structure and its surface properties deduced from ^{27}Al NMR and CO_2 IR characterization. Solid-state ^{27}Al NMR spectra indicate that as the calcination temperature increases, aluminum diffuses out of the brucite layers, incorporates into the octahedral and tetahedral positions of MgO, and thereby creates acid−base sites at the catalyst surface. CO_2 IR studies reveal that hydrotalcites calcined at 823 K exhibit a higher surface concentration of strong to medium basic sites than when calcined at 623 or 1273 K (Figure S9). Thus, the decreased catalytic activity for HT calcined at 623 K is a consequence of the lower amount of Al incorporated into the MgO lattice and the resulting decrease in the number of defect sites. On the other hand, the decrease in activity of HT calcined at 1273 K, which contains a spinel phase (Figure 1d), relates to the increased presence of Al−O^{2-} that has a much lower basicity than Mg−O^{2-} Lewis acid−base pairs.[26,38] The lower basicity of the spinel phase decreases the acetone conversion and results in the preferential formation of MO. Thus, the peak in propan-2-one conversion and selectivity to the cyclic trimer for a hydrotalcite calcination temperature of 823 K can be ascribed to the formation of new strong-medium basic sites by the substitution of aluminum into the MgO periclase structure.

The activity and selectivity of hydrotalcite (Mg/Al = 3) calcined at 823 K was also investigated for the dimerization and trimerization of C_4−C_5 methyl ketones. As seen in Figure 8, the conversions of butan-2-one and pentan-2-one are similar to that observed for propan-2-one, and high selectivities to cyclic trimer products are observed for each reactant. These findings are similar to those reported for batch trimerization of C_3−C_5 methyl ketones in the liquid phase.[6] The absence of oligomers higher than cyclic enone trimers is due to the steric hindrance around the reactive center of the molecule. It is notable that the conversion of pentan-3-one is lower and selectivity to the dimer product is >80%, suggesting that internal ketones are hard to condense further likely due to the lower acidity of the alpha hydrogen on the C_2 carbon of pentan-3-one and/or due to steric reasons.[43]

In situ IR spectroscopy was used to elucidate the mechanism for producing cyclic trimers from propan-2-one. As shown in Figure 9, pulsing propan-2-one over hydrotalcite (calcined at

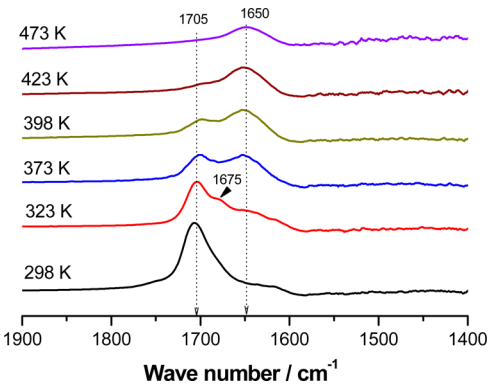

Figure 9. In situ FT-IR spectra of propan-2-one condensation over HT@823 K at various reaction temperatures.

823 K) at 298 K produces an intense peak at 1705 cm^{-1} characteristic of carbonyl (C═O) vibrations in propan-2-one (1730 cm^{-1} for gas-phase propan-2-one).[44] Increasing the temperature from 298 to 473 K results in a gradual disappearance of the peak at 1705 cm^{-1} and the appearance of peaks at 1675 and 1650 cm^{-1}. The peak at 1675 cm^{-1} appears at lower temperatures, and for temperatures above 373 K, the peak at 1650 cm^{-1} grows in and becomes the dominant feature in the spectrum. The peak at 1675 cm^{-1} is related to the formation of MO, whereas the peak at 1650 cm^{-1} relates to the cyclic trimer product, IP.[44] Peaks for aromatic compounds are not observed. These results suggest that mesityl oxide is an intermediate compound formed preferentially at lower temperatures (≤373 K). A similar result (not shown) was observed over (Mg/Al)O.

The IR results suggest that methyl ketones adsorption occurs through a Lewis acid−base interaction between the nucleophilic oxygen of the carbonyl group and the electrophilic metal species present on the catalyst surface. The strength of this interaction polarizes the carbonyl groups causing the carbon to become more electrophilic and the α-H to be more acidic. The increase in acidity facilitates α-H abstraction by the Brønsted basic oxygen to form bound water and an enolate intermediate. We envision that the ketones adsorb parallel to the oxide surface due to the strong interaction of α-H with the support

DOI: 10.1021/acs.iecr.6b03601
Ind. Eng. Chem. Res. 2016, 55, 10635−10644

surface. The function of the base sites on the hydrotalcites and (Mg/Al)O catalysts is, therefore, to abstract the proton in the α-position of propan-2-one. This process involves the formation of a carbanion intermediate that is further stabilized by the enolate isomer. Lewis acidic Al sites on hydrotalcites or (Mg/Al)O can further help to stabilize the negatively charged adsorbed intermediates. The polarization of another carbonyl bond induces nucleophilic attack by the enolate to the electrophilic carbon resulting in the formation of an aldol product, diacetone alcohol (DAA) (Scheme 2). DAA aldol readily undergoes dehydration to form the thermodynamically favored product, mesityl oxide. The dimer, mesityl oxide (MO), is thus the primary product in the self-condensation of propan-2-one following the rapid dehydration of unstable diacetone alcohol. Phorone and other acyclic trimeric intermediate structures are formed by the deprotonation of mesityl oxide in the α-position of the carbonyl function and its further condensation with a third propan-2-one molecule. The phorone undergoes rapid 1,6-Michael cyclization reaction in the presence of Lewis acidic sites to produce isophorone, which is a stable terminal product (Scheme 2).

α-H abstraction or carbon−carbon bond formation is considered to be the kinetically relevant rate limiting step in various aldol-type condensation reactions.[44,45] This hypothesis was tested by determining the kinetic isotope effects for the condensation reaction of propan-2-one. When deuterated propan-2-one ($(CD_3)_2CO$) was reacted over calcined hydrotalcite at 473 K, a kinetic isotope effect of k_H/k_D = 0.96 was observed, suggesting that the α C−H bond is not involved in the rate-limiting elementary step; rather carbon−carbon bond-formation is the critical step in methyl ketone condensation (Figure S10). Studies of the reaction kinetics thus indicate that the rate-determining step involves the condensation of the enolate intermediate with another molecule of propan-2-one to form DAA.[45]

The reaction kinetics for propan-2-one condensation were determined for HT and (Mg/Al)O calcined at 823 K. For both catalysts, the rate of reaction measured under differential conditions exhibited a 0.5 order dependence on the propan-2-one partial pressure and an activation energy of 37 kJ mol^{-1} in the temperature interval 453−493 K. The measured activation energy is in good agreement with the values (35−45 kJ mol^{-1}) reported for aldol condensation over various metal oxide and mixed oxide catalysts.[46,47] These results suggest that the active sites present on both catalysts are similar (Figure S11).

Previous studies have shown that the exposure of calcined hydrotalcite to water causes a loss of surface area, regeneration of Brønsted basicity, and reformation of the brucite-like structure of hydrotalcite.[16,17,48] It was, therefore, of interest to assess the effects of water on the stability of calcined hydrotalcite and (Mg/Al)O. For this purpose, the activity of (Mg/Al)O and HT@823 K was examined in the presence of 10 wt % water cofed together with propan-2-one. Figure 10 shows that after 150 min of time on stream, (Mg/Al)O shows negligible (<10%) activity loss, whereas calcined hydrotalcite loses 70% of its initial activity over the same period. Both catalysts were characterized after reaction in order to identify what changes had occurred. Data from XRD and ^{27}Al MAS NMR revealed that exposure of calcined hydrotalcite to water vapor restored its original layered structure (Figure S12). Restoration of the HT structure after rehydration implies that the Mg and Al phases are not fully segregated or phase separated as MgO and Al_2O_3 in HT@823 K catalysts.[49] Thus,

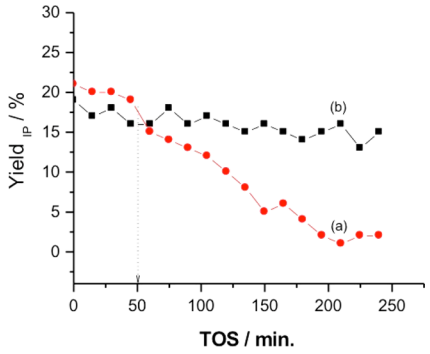

Figure 10. Water tolerant studies of (a) HT@823 K and (b) (Mg/Al)O catalysts in the presence and absence of water. The dotted line indicates the time at which 10 wt % water was cofed together with propan-2-one. Reaction conditions: T = 473 K, WHSV = 0.4 h^{-1}, M_{Cat} = 0.1 g, Q_{tot} = 150 cm^3 min^{-1}.

deactivation of calcined hydrotalcite catalysts is a consequence of restoration of the layered hydrotalcite structure by water produced during ketone condensation. By contrast, (Mg/Al)O is structurally robust and stable over the course of time on stream studies. All these results suggest that (Mg/Al)O catalysts have activities similar to those calcined hydrotalcites but have much higher water tolerance.

CONCLUSIONS

An in-depth investigation was conducted of the effects of composition and pretreatment of Mg−Al, acid−base catalysts for the self-condensation of biomass-derived C_3−C_5 methyl ketones. Catalysts containing weakly acidic and basic groups, such as calcined hydrotalcite and Al doped MgO, (Mg/Al)O, calcined at 823 K are found to exhibit the most promising catalytic properties for the trimerization of methyl ketones to cyclic enone trimers. Calcined hydrotalcites deactivate in the presence of water resulting in the restoration of the layered hydrotalcite structure, whereas (Mg/Al)O is structurally more robust in the presence of water. Characterization of calcined hydrotalcite by various techniques reveals that the relative abundance of strong, medium, and weak basic sites on the hydrotalcites depends on the temperature of catalyst pretreatments, and, in general, the presence of strong-medium basic sites increases with an increase in catalyst pretreatment. Spectroscopic studies suggest that upon calcination, aluminum diffuses out of the brucite layers and substitutes into the tetrahedral and octahedral sites of the MgO matrix producing new Lewis acid−base pairs. Hydrotalcites pretreated at 623 and 1273 K exhibit decreased basicity and showed preferential condenation of methyl ketones to form acyclic dimer enones, whereas calcination at 823 K promotes the selective formation of cyclic enone trimers. These findings suggest that an optimum concentration of acid−base sites is necessary to promote selective trimerization. (Mg/Al)O calcined at 823 K exhibits characteristics very similar to those of HT calcined at 823 K. In this case, Al^{3+} cations diffuse into the tetrahedral and octahedral sites of the MgO cyrstallites and produce new Lewis acid−base pairs. Consistent with this interpretation, (Mg/Al)O calcined at 823 K is found to exhibit catalytic activity and selectivity nearly identical to that of hydrotalcite calcined at 823 K. H/D isotopic tracer studies reveal that the C−C bond formation step be the rate-limiting step in the self-condensation of methyl ketones.

DOI: 10.1021/acs.iecr.6b03601
Ind. Eng. Chem. Res. 2016, 55, 10635−10644

■ ASSOCIATED CONTENT

Supporting Information

The Supporting Information is available free of charge on the ACS Publications website at DOI: 10.1021/acs.iecr.6b03601.

Thermogravimetric analysis, textural properties, elemental mapping, ^{25}Mg MAS NMR, pyridine-CO_2 IR, XRD, and kinetic studies of calcined hydrotalcite and (Mg/Al)O oxide catalyst (PDF)

■ AUTHOR INFORMATION

Corresponding Author

*Phone: +1 510 642 1536. Fax +1 510 642 4778. E-mail: bell@cchem.berkeley.edu.

Notes

The authors declare no competing financial interest.

■ ACKNOWLEDGMENTS

This work was supported by the Energy Bioscience Institute. STEM-EDS mapping was performed at the National Center for Electron Microscopy at the Molecular Foundry, Lawrence Berkeley National Laboratory. Work at the Molecular Foundry was supported by the Office of Science, Office of Basic Energy Sciences, of the U.S. Department of Energy under Contract No. DE-AC02-05CH11231. We gratefully acknowledge the contributions of Dr. Benjamin Keitz and Dr. Gregory Johnson to the characterization section of the manuscript.

■ REFERENCES

(1) Huber, G. W.; Chheda, J. N.; Barrett, C. J.; Dumesic, J. A. Production of Liquid-Alkanes by Aqueous Phase Processing of Biomass-Derived Carbohydrates. *Science* **2005**, *308*, 1446.

(2) Huber, G. W.; Iborra, S.; Corma, A. Synthesis of Transportation Fuels from Biomass: Chemistry, Catalysts, and Engineering. *Chem. Rev.* **2006**, *106*, 4044.

(3) Corma, A.; de La Torre, O.; Renz, M.; Villandier, N. Production of High-Quality Diesel from Biomass Waste Products. *Angew. Chem., Int. Ed.* **2011**, *50*, 2375.

(4) Corma, A.; de La Torre, O.; Renz, M. Production of High Quality Diesel from Cellulose and Hemicellulose by the Sylvan Process: Catalysts and Process Variables. *Energy Environ. Sci.* **2012**, *5*, 6328.

(5) Bond, J. Q.; Alonso, D. M.; Wang, D.; West, D.; Dumesic, J. A. Integrated Catalytic Conversion of γ-Valerolactone to Liquid Alkenes for Transportation Fuels. *Science* **2010**, *327*, 1110.

(6) Sacia, E. R.; Balakrishnan, M.; Deaner, M. H.; Goulas, K. A.; Toste, F. D.; Bell, A. T. Highly Selective Condensation of Biomass-Derived Methyl Ketones as a Source of Aviation Fuel. *ChemSusChem* **2015**, *8*, 1726.

(7) Anbarasan, P.; Baer, Z. C.; Sreekumar, S.; Gross, E.; Binder, J. B.; Blanch, H. W.; Clark, D. S.; Toste, F. D. Integration of Chemical Catalysis with Extractive Fermentation to Produce Fuels. *Nature* **2012**, *491*, 235.

(8) Ji, X.-J.; Huang, H.; Ouyang, P. K. Microbial 2,3-Butanediol Production: a State-of-the-art Review. *Biotechnol. Adv.* **2011**, *29*, 351.

(9) Multer, A.; McGraw, N.; Hohn, K.; Vadlani, P. Production of Methyl Ethyl Ketone from Biomass Using a Hybrid Biochemical/Catalytic Approach. *Ind. Eng. Chem. Res.* **2013**, *52*, 56.

(10) Gong, Y.; Lin, L.; Shi, J. B.; Liu, S. J. Oxidative Decarboxylation of Levulinic Acid by Cupric Oxides. *Molecules* **2010**, *15*, 7946.

(11) Hanna, D. G.; Shylesh, S.; Li, Y.-P.; Krishna, S.; Head-Gordon, M.; Bell, A. T. Experimental and Theoretical Study of n-Butanal Self-Condensation Over Ti Species Supported on Silica. *ACS Catal.* **2014**, *4*, 2908.

(12) Shylesh, S.; Sreekumar, S.; Gomes, J.; Head-Gordon, M.; Toste, F. D.; Bell, A. T.; Grippo, A.; Arab, G. E. Catalytic Upgrading of Biomass-Derived Methyl Ketones to Liquid Transportation Fuel Precursors by an Organocatalytic Approach. *Angew. Chem., Int. Ed.* **2015**, *54*, 4673.

(13) Balakrishnan, M.; Sacia, E. R.; Sreekumar, S.; Gunbas, G.; Gokhale, A. A.; Scown, C. D.; Toste, F. D.; Bell, A. T. Novel Pathways for Fuels and Lubricants from Biomass Optimized Using Life-Cycle Greenhouse Gas Assessment. *Proc. Natl. Acad. Sci. U. S. A.* **2015**, *112*, 7645.

(14) Hattori, H. Heterogeneous Basic Catalysis. *Chem. Rev.* **1995**, *95*, 537.

(15) Renfrow, W. B.; Renfrow, A. A Study of Alternate Methods for the Alkylation of Aetoacetic Esters. *J. Am. Chem. Soc.* **1946**, *68*, 1801.

(16) Cavani, F.; Trifiro, F.; Vaccari, A. Hydrotalcite-type Anionic Clays: Preparation, Properties and Applications. *Catal. Today* **1991**, *11*, 173 and references therein..

(17) Nishimura, S.; Takagaki, A.; Ebitani, N. Characterization, Synthesis and Catalysis of Hydrotalcite-Related Materials for Highly Efficient Materials Transformations. *Green Chem.* **2013**, *15*, 2026 and references therein..

(18) van Bokhoven, J. A.; Roelofs, J. C. A. A.; de Jong, K. P.; Koningsberger, D. C. Unique Structural Properties of the Mg-Al Hydrotalcite Solid Base Catalyst: An In Situ Study Using Mg and Al K-Edge XAFS during Calcination and Rehydration. *Chem. - Eur. J.* **2001**, *7*, 1258.

(19) Sideris, P. J.; Nielsen, V. G.; Gan, Z.; Grey, C. P. Mg/Al Ordering in Layered Double Hydroxides Revealed by Multinuclear NMR Spectroscopy. *Science* **2008**, *321*, 113.

(20) Choudary, B. M.; Kantam, M. L.; Reddy, C. V.; Rao, K. K.; Figuearas, F. The First Example of Michael Addition Catalysed by Modified Mg-Al Hydrotalcite. *J. Mol. Catal. A: Chem.* **1999**, *146*, 279.

(21) Prescott, H. A.; Li, Z.-J.; Kemnitz, E.; Trunschke, A.; Deutsch, J.; Lieske, H.; Auroux, A. Application of Calcined Mg-Al Hydrotalcites for Michael Additions: An Investigation of Catalytic Activity and Acid-Base Properties. *J. Catal.* **2005**, *234*, 119.

(22) Climent, M. J.; Corma, A.; Iborra, S.; Primo, J. Base Catalysis for Fine Chemicals Production: Claisen-Schmidt Condensation on Zeolites and Hydrotalcites for the Production of Chalcones and Flavanones of Pharmaceutical Interest. *J. Catal.* **1995**, *151*, 60.

(23) Diez, V. K.; Apesteguia, C. R.; DiCosimo, J. I. Effect of the Chemical Composition on the Catalytic Performance of Mg_yAlO_x Catalysts for Alcohol Elimination Reactions. *J. Catal.* **2003**, *215*, 220.

(24) Liu, Y.; Lotero, E.; Goodwin, J. G.; Mo, X. Transesterification of Poultry Fat with Methanol Using Mg-Al Hydrotalcite Derived Catalysts. *Appl. Catal., A* **2007**, *331*, 138.

(25) Kanezaki, E. Direct Observation of a Metastable Solid Phase of $Mg/Al/CO_3$-Layered Double Hydroxide by Means of High Temperature in Situ Powder XRD and DTA/TG. *Inorg. Chem.* **1998**, *37*, 2588.

(26) Vrieland, G. E.; Khazai, B.; Murchison, C. B. Anaerobic Oxidation of Butane to Butadiene Over Magnesium Molybdate Catalysts. II. Magnesia Alumina Supported Catalysts. *Appl. Catal., A* **1996**, *134*, 123.

(27) Shen, J.; Kobe, J. M.; Chen, Y.; Dumesic, J. A. Synthesis and Surface Acid/Base Properties of Magnesium-Aluminum Mixed Oxides Obtained from Hydrotalcites. *Langmuir* **1994**, *10*, 3902.

(28) MacKenzie, K. J. D.; Meinhold, R. H.; Sherriff, B. L.; Xu, Z. ^{27}Al and ^{25}Mg Solid-Sate Magic-Angle Spinnng Nuclear Magnetic Resonance Study of Hydrotalcite and its Thermal Decomposition Sequence. *J. Mater. Chem.* **1993**, *3*, 1263.

(29) Pesic, L.; Salipurovic, S.; Markovic, V.; Vucelic, D.; Kagunya, W.; Jones, W. Thermal Characteristics of a Synthetic Hydrotalcite-like Material. *J. Mater. Chem.* **1992**, *2*, 1069.

(30) Corma, A.; Fornes, V.; Rey, F. Hydrotalcites as Base Catalysts: Influence of the Chemical Composition and Synthesis Conditions on the Dehydrogenation of Isopropanol. *J. Catal.* **1994**, *148*, 205.

(31) Frydman, L.; Harwood, J. S. Isotropic Spectra of Half-Integer Quadrupolar Spins from Bidimensional Magic-Angle Spinning NMR. *J. Am. Chem. Soc.* **1995**, *117*, 5367.

(32) Medek, A.; Harwood, J. S.; Frydman, L. Multiple-Quantum Magic-Angle Spinning NMR: A New Method for the Study of Quadrupolar Nuclei in Solids. *J. Am. Chem. Soc.* **1995**, *117*, 12779.

DOI: 10.1021/acs.iecr.6b03601
Ind. Eng. Chem. Res. 2016, 55, 10635−10644

(33) Rocha, J.; del Arco, M.; Rives, V.; Ulibarri, M. A. Reconstruction of Layered Double Hydroxides from Calcined Precursors: a Powder XRD and ^{27}Al MAS NMR Study. *J. Mater. Chem.* **1999**, *9*, 2499.
(34) Shen, J.; Tu, M.; Hu, C. Structural and Surface Acid/Base Properties of Hydrotalcite-Derived MgAlO Oxides Calcined at Varying Tempertaures. *J. Solid State Chem.* **1998**, *137*, 295.
(35) Pallister, P. J.; Moudrakovski, I. L.; Ripmeester, J. A. Mg-25 Ultra-High Field Solid State NMR Spectroscopy and First Principles Calculations of Magnesium Compounds. *Phys. Chem. Chem. Phys.* **2009**, *11*, 11487.
(36) MacKenzie, K. J. D.; Meinhold, R. H. Thermal Decomposition of Brucite, $Mg(OH)_2$: a ^{25}Mg MAS NMR Study. *Thermochim. Acta* **1993**, *230*, 339.
(37) Kawakami, H.; Yoshida, S. Theoretical Approach to the Basicity of Alkaline-Earth-Metal Oxide Catalysts. Relationship Between Basicity and Surface Structure of Magnesium Oxide. *J. Chem. Soc., Faraday Trans. 2* **1984**, *80*, 921.
(38) Di Cosimo, J.; Diez, V. K.; Xu, M.; Iglesia, E.; Apesteguia, C. R. Structure and Surface and Catalytic Properties of Mg-Al Basic Oxides. *J. Catal.* **1998**, *178*, 499.
(39) Busch, O. M.; Brijoux, W.; Thomson, S.; Schuth, F. Spatially Resolving Infrared Spectroscopy for Parallelized Characterization of Acid Sites of Catalysts via Pyridine Sorption: Possibilities and Limitations. *J. Catal.* **2004**, *222*, 174.
(40) Salvapati, G. S.; Ramanamurty, K. V.; Janardanarao, M. Selective Catalytic Self-Condensation of Acetone. *J. Mol. Catal.* **1989**, *54*, 9.
(41) Di Cosimo, J. I.; Diez, V. K.; Apesteguia, C. R. Synthesis of Unsaturated Ketones over Thermally Activated Mg-Al Hydrotalcites. *Appl. Clay Sci.* **1998**, *13*, 433.
(42) Ramasamy, K. K.; Gray, M.; Job, H.; Smith, C.; Wang, Y. Tunable Catalytic Properties of Bi-functional Mixed Oxides in Ethanol Conversion to High Value Compounds. *Catal. Today* **2016**, *269*, 82.
(43) Baylon, R. A. L.; Sun, J.; Martin, K. J.; Venkitasubramanian; Wang, Y. Beyond Ketonization: Selective Conversion of Carboxylic Acids to Olefins over Balanced Lewis Acid-Base Pairs. *Chem. Commun.* **2016**, *52*, 4975.
(44) Quesada, J.; Faba, L.; Diaz, E.; Bennici, S.; Auroux, A.; Ordonez, S. Role of Surface Intermediates in the Deactivation of Mg-Zr Mixed Oxides in Acetone Self-Condensation: A Combined DRIFT and ex situ Characterization Approach. *J. Catal.* **2015**, *329*, 1.
(45) Reichle, W. T. Pulse Microreactor Examination of the Vapor-Phase Aldol Condensation of Acetone. *J. Catal.* **1980**, *63*, 295.
(46) Rekoske, J. E.; Barteau, M. A. Kinetics, Selectivity and Deactivation in the Aldol Condensation of Acetaldehyde on Anatase Titanium Dioxide. *Ind. Eng. Chem. Res.* **2011**, *50*, 41.
(47) McKenzie, A. I.; Fishel, C. T.; Davis, R. J. Investigation of the Surface Structure and Basic Properties of Calcined Hydrotalcites. *J. Catal.* **1992**, *138*, 547.
(48) Corma, A.; Hamid, S. B. A.; Iborra, S.; Velty, A. Lewis and Bronsted Basic Active Sites on Solid Catalyst and Their Role in the Synthesis of Monoglycerides. *J. Catal.* **2005**, *234*, 340.
(49) Jiang, D.; Zhao, B.; Xie, Y.; Pan, G.; Ran, G.; Min, E. Structure and Basicity of γ-Al_2O_3-Supported MgO and its Application to Mercaptan Oxidation. *Appl. Catal., A* **2001**, *219*, 69.

DOI: 10.1021/acs.iecr.6b03601
Ind. Eng. Chem. Res. 2016, 55, 10635−10644